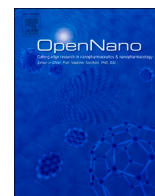


## Lab-scale siRNA and mRNA LNP manufacturing by various microfluidic mixing techniques - an evaluation of particle properties and efficiency

David C. Jürgens, Leonie Deßloch, Diana Porras-Gonzalez, Joshua Winkeljann, Sebastian Zielinski, Matthias Munschauer, Andreas L. Hörner, Gerald Burgstaller, Benjamin Winkeljann, Olivia M. Merkel

### Angaben zur Veröffentlichung / Publication details:

Jürgens, David C., Leonie Deßloch, Diana Porras-Gonzalez, Joshua Winkeljann, Sebastian Zielinski, Matthias Munschauer, Andreas L. Hörner, Gerald Burgstaller, Benjamin Winkeljann, and Olivia M. Merkel. 2023. "Lab-scale siRNA and mRNA LNP manufacturing by various microfluidic mixing techniques - an evaluation of particle properties and efficiency." OpenNano 12: 100161. <https://doi.org/10.1016/j.onano.2023.100161>.



# Lab-scale siRNA and mRNA LNP manufacturing by various microfluidic mixing techniques – an evaluation of particle properties and efficiency

David C. Jürgens<sup>a</sup>, Leonie Deßloch<sup>a</sup>, Diana Porras-Gonzalez<sup>c</sup>, Joshua Winkeljann<sup>d</sup>, Sebastian Zielinski<sup>e,f,g</sup>, Matthias Munschauer<sup>e,f,g</sup>, Andreas L. Hörner<sup>d</sup>, Gerald Burgstaller<sup>c</sup>, Benjamin Winkeljann<sup>a,b</sup>, Olivia M. Merkel<sup>a,b,c,\*</sup>

<sup>a</sup> Department of Pharmacy, Ludwig-Maximilians-University Munich, Butenandtstrasse 5-13, Haus B, Munich 81377, Germany

<sup>b</sup> Center for NanoScience (CeNS), Ludwig-Maximilians-University Munich, Munich 80799, Germany

<sup>c</sup> Member of the German Center for Lung Research (DZL), Comprehensive Pneumology Center (CPC) with the CPC-M bioArchive/Institute of Lung Health and Immunity (LHI), Helmholtz Zentrum München, Munich, Germany

<sup>d</sup> Department of experimental Physics, University of Augsburg, Universitätsstraße 1, Augsburg 86159, Germany

<sup>e</sup> Helmholtz Institute for RNA-based Infection Research, Helmholtz Center for Infection Research, Würzburg, Germany

<sup>f</sup> Josef-Schneider-Straße 2/D15, Würzburg D-97080, Germany

<sup>g</sup> University of Würzburg, Medical Faculty, Josef-Schneider-Straße 2/D15, D-97080, Würzburg, Germany

## ARTICLE INFO

### Keywords:

siRNA  
mRNA  
LNP  
Microfluidics  
Lab-scale

## ABSTRACT

Lipid Nanoparticles (LNPs) are promising drug delivery systems for various RNAs such as small interfering (siRNA) and messenger RNA (mRNA). Microfluidic mixing is a common technique to encapsulate RNA in LNPs. However, high flow rates and lipid concentrations are used for LNP formation to control LNP size as well as RNA encapsulation efficiency. We investigated the feasibility of downscaling siRNA and mRNA LNP manufacturing to save materials and enable a broader access to this technology. To optimize such a down-scaled procedure, we evaluated physicochemical nanoparticle characteristics including hydrodynamic diameter, zeta potential, particle concentration, encapsulation efficiency, and recovery for LNPs produced with three different microfluidic methods. We observed differences in nanoparticle characteristics and *in vitro* performance regarding cellular uptake, gene silencing, and mRNA expression. We determined the gene knockdown ability of the best siRNA LNPs formulation *ex vivo* using precision-cut lung slices to highlight the translational character of LNPs for inhalation and observed comparable efficacy as with a commercially available transfection reagent.

## 1. Introduction

In 2018, the European Medicines Agency (EMA) and the U.S. Food and Drug Administration (FDA) approved the first Lipid Nanoparticle (LNP)-based RNA drug, Onpatro®, which revolutionized the treatment of hereditary transthyretin amyloidosis (hATTR) with small interfering RNA (siRNA) [1]. In 2021, the approval of the first messenger RNA (mRNA) formulations for vaccination against

\* Corresponding author at: Department of Pharmacy, Ludwig-Maximilians-University Munich, Butenandtstrasse 5-13, Haus B, Munich 81377, Germany.

E-mail address: [olivia.merkel@lmu.de](mailto:olivia.merkel@lmu.de) (O.M. Merkel).

<https://doi.org/10.1016/j.onano.2023.100161>

Received 27 February 2023; Received in revised form 3 May 2023; Accepted 4 May 2023

Available online 8 May 2023

2352-9520/© 2023 The Author(s). Published by Elsevier Inc. This is an open access article under the CC BY-NC-ND license (<http://creativecommons.org/licenses/by-nc-nd/4.0/>).

SARS-CoV-2 by Moderna and BioNTech/Pfizer marked the next milestone in the story of LNP-based drug delivery. Both companies showed that their LNP formulations can transfect cells at the site of action [2]. The manufacturing process for LNPs in literature follows mostly the same pattern with the lipids being solubilized in ethanol and mixed with an acidic aqueous RNA solution using microfluidics. After this pre-assembly, a buffer exchange is applied to obtain the final nanoparticle [3]. The physicochemical properties of the LNPs are mainly determined by the lipid composition, lipid concentration, mixing method, total flow rates (TFR), flow rate ratio (FRR), and excipient-to-RNA ratio [4–6]. Companies such as Precision NanoSystems, Knauer or Elveflow offer microfluidic-based devices for optimized LNP production and thus offer research institutes and pharmaceutical industry access to the formulation procedure. Interestingly, the devices offered by these three companies support the manufacturing of LNPs with high flow rates in the ml/min scale, which is reflected by many publications in the field [4,7–11]. The aim of this study is to investigate the feasibility of downsizing the manufacturing of siRNA and mRNA-loaded LNPs. Small-scale LNP production is of particular relevance for academic research, as the need for customized formulations and the limited availability of funding often requires the use of smaller volumes. Moreover, small-scale production can reduce waste of materials enabling more efficient screening of different LNP formulation parameters. This facilitates the identification of the most promising formulation candidates for further investigation and scale-up. We here focused on the Onpattro-based formulation which is known to deliver siRNA and mRNA successfully both *in vitro* and *in vivo* [4, 12]. Most LNP formulations are comprised of an ionizable lipid, a PEGylated lipid, cholesterol, and a helper lipid in a defined ratio, as the interplay of these lipids leads to functional LNPs. The ionizable lipid can thereby interact electrostatically with nucleic acids at low pH during the microfluidic assembly and facilitates membrane fusion *in vitro* [2]. The helper lipid and cholesterol have different functions, including RNA encapsulation and cellular delivery [13]. The PEGylated lipid is necessary to prevent opsonization *in vivo* and to control particle size by steric hindrance [14].

In order to assess the feasibility of downscaling the production of LNPs, we conducted an investigation into the physicochemical properties and cellular efficiency of LNPs formulated using three distinct microfluidic mixing techniques: staggered Herringbone mixing, T-junction mixing, and hydrodynamic flow focusing (HFF). T-junction mixing involves the mixing of two fluids at a T-junction, where one fluid flows perpendicularly into the other, creating a rapidly mixing flow. Staggered Herringbone mixing is a method, in which the sample flows through a series of staggered ridges and grooves, causing advection and mixing of the sample. Hydrodynamic flow focusing, on the other hand, uses two streams of fluid, one sheath fluid and one sample fluid, flowing in parallel and at different flow rates through a microchannel. The higher flow rate of the sheath fluid, when compared to the sample fluid's flow rate, causes the sample fluid to be focused into a narrow stream where mixing at the interface between sample and sheath fluid can be facilitated. Each of these methods has unique advantages and disadvantages, and the choice of method may depend on the desired properties of the final lipid nanoparticle formulation. Our goal was to achieve sizes below or near 100 nm based on the particle size reported in the Onpattro EMA public assessment report and studies conducted on mRNA transfection efficiency [10]. While studies on total flow rate in laminar and turbulent mixing influence, as well as the speed at which the critical ethanol concentration range is crossed, have been described, cellular experiments are lacking [5,15,16]. Thus, we here investigated the cellular uptake, mRNA expression, and GFP silencing capability of mRNA- and siRNA-loaded LNPs, respectively. As the goal of this study was to provide an overview of suitable methods for lab-scale LNP manufacturing, variations in lipid composition and LNP morphology were not investigated.

This study provides an overview of the mixing methods on LNP formation with low flow rates and broad nanoparticle characterization of the formulated LNPs. Finally *in vitro* and *ex vivo* performance testing was conducted, confirming the efficacy of low flow-rate manufactured LNPs.

## 2. Material and methods

### 2.1. Production of mRNA

DNA template for *in vitro* transcription (IVT) was generated by subcloning eGFP flanked with previously described UTR sequences [17] into the pCR4-TOPO backbone (Thermo Fisher Scientific, Darmstadt, Germany). DNA was digested with NotI-HF (New England Biolabs, Frankfurt am Main, Germany) and linearized DNA template was used for IVT reactions using 20 ng/μl T7 RNA polymerase HC (Jena Bioscience, Jena, Germany), with equimolar ratios of all natural ribonucleotides. The complete IVT mixture was incubated at 37 °C for 2.5 h. Thereafter, DNase I (New England Biolabs, Frankfurt am Main, Germany) (40 U/ml) was used to digest the residual DNA template for another 30 min at 37 °C. Resulting mRNA was dephosphorylated using Quick CIP (40 U/ml) (New England Biolabs, Frankfurt am Main, Germany) at 37 °C for 20 min. RNA was purified by precipitation, and the pellet was reconstituted in RNase-free water. For co-transcriptional capping of mRNA, the proportion of rGTP in the reaction mixture was adjusted (20% rGTP, 80% ARCA) to ensure efficient capping.

### 2.2. Fluorescent labeling of mRNA

To fluorescently label mRNA, the Mirus labeling Cy5-Kit (#MIR 3700, Madison, USA) was used. Labeling was performed according to the manufacturer's recommendations with the following modifications: the ratio of fluorescent dye and mRNA was adapted in order to achieve an approximately 10-fold lower labeling density resulting in a calculated overall base to dye ratio of 560:1.

### 2.3. Preparation of siRNA and mRNA-loaded LNPs

The small interfering RNA (siRNA) LNP and messenger RNA (mRNA) LNP formulations are based on the lipid composition of the

**Table 1**  
siRNA sequences.

Name	Sense strand (5'-3')	Antisense strand (3'-5')
siGFP	pACC <u>CUGAAGU</u> UCAUCGACCACcg	ACUGGGACUCCAAGUAGACGGGUGGC
siNC	pCGUUAAUCGCGUAUAAUACGCGUat	CAGCAAUUAGCGCAUAAUUAUGCGCAUAp
siGAPDH	pAGCAUCUCCUCACAAUUUCCAUcc	ACUCGUAGAGGGAGUGUAAAAGGUAGG

The letter p denotes a phosphate residue, lower case bold letters are 2-deoxyribonucleotides, capital letters are ribonucleotides and underlined capital letters are 2-O-methylribonucleotides.

clinically approved Onpatro® formulation. Thus, ionizable lipid (6Z,9Z,28Z,31Z)-heptatriaconta-6,9,28,31-tetraen-19-yl 4-(dimethylamino)butanoate (Dlin-MC3-DMA, MedChemExpress, Monmouth Junction, USA) a helper lipid 1, 2-distearoyl-sn-glycero-3-phosphocholine (DSPC, Sigma Aldrich, Taufkirchen, Germany), cholesterol (Corden Pharma, Taufkirchen, Germany) and the PEGylated lipid 1,2-dimyristoyl-rac-glycero-3-methoxypolyethylene glycol-2000 (DMG-PEG 2000, Sigma Aldrich, Taufkirchen, Germany) were dissolved in ethanol and diluted to a final concentration of 1 mM. Afterwards, the lipids were mixed in a molar ratio of 50:10:38.5:1.5 mol%. For aqueous RNA solutions, siRNA and mRNA were separately dissolved in 25 mM sodium acetate buffer (pH 4) according to a nitrogen-to-phosphate (N/P) ratio of 3 for siRNA and an N/P ratio of 6 for mRNA. The N/P ratio in general describes the ratio of the amine group within the ionizable lipid to the phosphate groups of the siRNA backbone.

The two solutions were mixed at a total flow rate (TFR) of 5 mL/h and a flow rate ratio (FRR) of 3:1 V/V (aqueous/organic phase) at 21 °C. The siRNA-LNPs and mRNA-LNPs were prepared with 0.38 mm polyethylene tubings (Becton, Dickinson and Company, Parsippany, USA) using a T-junction mixer, staggered Herringbone mixing microfluidic chip (Fluidic 187, Microfluidic ChipShop, Jena, Germany) and hydrodynamic flow focusing (HFF) manufactured in-house, respectively. For HFF, a polydimethylsiloxane (PDMS) microchannel was fabricated using soft lithography techniques. The inlets have a circular shape with a diameter of 1 mm, whereas the channel itself has a rectangular shape of 300 µm in width and 100 µm in height. The whole channel has a length of 22 mm. After microfluidic mixing, final LNPs were obtained by dialysis (3.5 kDa Pur-A-Lyzer™ Maxi Dialysis kit, Sigma Aldrich, Taufkirchen, Germany) over night against sterile PBS (Thermo Fisher Scientific, Darmstadt, Germany) pH 7.4 at 4 °C and sterile filtration using 0.22 µm Acrodisc® syringe filter (Pall, Dreieich, Germany). After dialysis, an increase of volume was observed. The factor of volume increase was determined for each sample and used for further analysis on LNP recovery and encapsulation efficiency. All siRNA duplexes, including fluorescently labeled ones, used were obtained from Integrated DNA Technologies (IDT, Leuven, Belgium), and their sequences are listed in Table 1.

#### 2.4. Hydrodynamic diameters and zeta potentials of siRNA and mRNA-loaded LNPs

Hydrodynamic diameter and polydispersity index (PDI) were determined by dynamic laser scattering (DLS) in disposable cuvettes (Malvern Instruments, Malvern, UK) using a Zetasizer Advance Ultra (Malvern Instruments, Malvern, UK) with backscatter angle detection at 21 °C. LNP samples were prepared as described above using scrambled siRNA (Integrated DNA Technologies, Leuven, Belgium) and uncapped eGFP mRNA, respectively. For measurements, LNPs were diluted 1:10 with PBS. Measurements were performed in triplicates ( $n = 3$ ). Data analysis was performed by ZS Xplorer software (v. 3.2.0). Results are given as average size (nm)  $\pm$  SD.

Mean, Modus, Span, and particle count were evaluated by nanoparticle tracking analysis (NTA) at 21 °C. Here, respective samples were diluted 1:100 and injected into the device using the syringe pump of the Nanosight NS300 (Malvern Instruments, Malvern, UK) according to the manufacture instructions. Measurements were performed in triplicates ( $n = 3$ ). Results are given as mean, modus, and span (nm)  $\pm$  SD. Particle concentration is given as particles/ml  $\pm$  SD.

Zetapotential was measured by laser doppler anemometry (LDA) using a Zetasizer Advance Ultra (Malvern Instruments, Malvern, UK). Of each formulation 100 µL was diluted 1:7 with highly purified water and transferred to a non-disposable capillary cell (Malvern Instruments, Malvern, UK). Data analysis was performed by ZS Xplorer software (v. 3.2.0) and given as average charge (mV)  $\pm$  SD. Measurements were performed in triplicates with 30 runs for each sample. ( $n = 3$ )

#### 2.5. Recovery and encapsulation efficiency

For total RNA recovery and LNP encapsulation efficiency Quant-iT™ RiboGreen™ (Invitrogen™, Thermo Fisher Scientific, Schwerte, Germany) was used. LNP samples were prepared as described above using scrambled siRNA (Integrated DNA Technologies, Leuven, Belgium) and uncapped eGFP mRNA, respectively. Briefly, 50 µL of samples were transferred into a black 96-well plate and filled up to 100 µL either with TE buffer (Sigma Aldrich, Taufkirchen, Germany) pH 7.5 for encapsulation efficiency or 2% Triton X-100 (Sigma Aldrich, Taufkirchen, Germany) in TE buffer solution for total RNA recovery. Standard curves were prepared in both solutions by 5 serial dilutions of 10 µg/ml siRNA and 6,75 µg/ml mRNA, respectively. The plate was incubated in a shaking incubator at 37 °C for 60 min. To each well, 100 µL of the fluorescent dye Ribogreen™ at a dilution of 1:100 was added. The fluorescence intensity was measured after 10 min at an excitation wavelength of 480 nm and emission wavelength of 525 nm at a microplate plate reader (Tecan Spark, TECAN, Maennedorf, Switzerland). Results are given as percentage  $\pm$  SD. Measurements were performed in technical duplicates ( $N = 3$ ).

## 2.6. Cell culture

The human non-small cell lung carcinoma cell line H1299 (ATCC, VA, USA) and stably eGFP plasmid transfected H1299 reporter cells (H1299-GFP) were cultured in RPMI media (Sigma Aldrich, Taufkirchen, Germany) supplemented with heat-inactivated FBS (10%, Thermo Fisher Scientific, Darmstadt, Germany), and Penicillin-Streptomycin (1%, Thermo Fisher Scientific, Darmstadt, Germany) in PBS (Thermo Fisher Scientific, Darmstadt, Germany). For H1299-GFP cells, additional 0,4% G-418 solution (98%, Sigma Aldrich, Taufkirchen, Germany) was added to the growth medium. All cells were subcultured, maintained, and grown in an incubator (humidified air with 5% CO<sub>2</sub> at 37 °C) and split every 3 days to reach confluency upon further experiments.

## 2.7. Cellular uptake and mRNA expression

For cellular uptake and mRNA expression experiments, 50,000 H1299 cells in 500 µL growth medium were seeded in a 24-well plate and incubated (humidified air with 5% CO<sub>2</sub> at 37 °C) for 24 h upon transfection. LNPs were formulated with AF488-labeled siRNA (Integrated DNA Technologies, Leuven, Belgium) and Cy5-labeled eGFP mRNA by applying T-junction mixing, staggered Herringbone mixing and HFF, respectively, as described above. For transfection, LNPs were diluted in sterile PBS for a final dose of 50 pmol siRNA and 100 ng mRNA in 100 µL prior to transfection based on encapsulated RNA. For blank samples 100 µL of sterile PBS was added to each well. Positive controls were prepared by using Lipofectamine 2000 (Thermo Fisher Scientific, Darmstadt, Germany) for siRNA and Lipofectamine Mmax (Thermo Fisher Scientific, Darmstadt, Germany) for mRNA, according to the manufacturer's instruction based on used siRNA and mRNA LNP doses. After 24 h, medium was aspirated and cells were washed with PBS. Afterwards, 100 µL 0.1% trypsin (Thermo Fisher Scientific, Darmstadt, Germany) was added for 5 min to detach the cells. Trypsinization was stopped using 300 µL complete growth medium. The cell suspensions were transferred to 1,5 ml Eppendorf tubes and centrifuged (400 rcf, 5 min, 21 °C). After centrifugation the supernatant was aspirated, cells were washed twice using 500 µL PBS (400 rcf, 5 min, 21 °C), and resuspended in 400 µL PBS containing 2 mmol EDTA (Sigma Aldrich, Taufkirchen, Germany) (400 rcf, 5 min, 21 °C). Cell suspensions of samples treated with AF488-labeled siRNA LNPs were mixed before measurement with an equal volume of 0.4% trypan blue solution (Thermo Fisher Scientific, Darmstadt, Germany) to quench extracellular fluorescence. Flow cytometry (Attune Nxt, Thermo Fisher Scientific, Darmstadt, Germany) was performed gating 10,000 cells using a 488 nm excitation laser with BL1 filter for samples treated with LNPs loaded with AF488-labeled siRNA. For mRNA cellular uptake and expression, 488 nm and 638 nm excitation laser with BL1 and RL1 filters were used simultaneously. Datapoints are given as MFI average of 3 replicates ± SD (N = 3).

## 2.8. GFP knockdown

For gene silencing experiments, 25,000 H1299-eGFP cells in 500 µL were seeded in a 24-well plate and incubated (humidified air with 5% CO<sub>2</sub> at 37 °C) for 24 h upon transfection. LNPs were formulated with eGFP siRNA (Integrated DNA Technologies, Leuven, Belgium) by applying T-junction mixing, staggered Herringbone mixing and HFF. Dilution of LNPs for a final dose of 50 pmol siRNA treatment of blank samples, and positive controls were performed as described above. After 48 h, sampling was conducted as described above. Flow cytometry was performed gating 10,000 cells using a 488 nm excitation laser with BL1 filter. Datapoints are given as MFI average of 3 replicates ± SD (N = 3).

## 2.9. Confocal microscopy

For confocal microscopy 50,000 H1299 cells were seeded on a coverslip in a 24-well plate. LNPs were formulated with AF488-labeled siRNA (Integrated DNA Technologies, Leuven, Belgium) by HFF and transfection was performed with 50 pmol siRNA as described above. After 24 h, medium was aspirated and cells were washed 3 times with ice-cold PBS. Afterward, cells were fixed using 4% paraformaldehyde (PFA, 37%, Sigma Aldrich, Taufkirchen, Germany) for 15 min at 4 °C. Residual PFA was removed by washing three times with ice-cold PBS. After fixation, nuclei were stained applying a treatment with 0.5 µg/ml 4',6-Diamidin-2-phenylindol (DAPI, Thermo Fisher Scientific, Darmstadt, Germany) in PBS for 15 min in dark at 4 °C. Thereafter, cells were washed 3 times with PBS and mounted onto a coverslip using Fluorsafe reagent (VWR, Ismaning, Germany) for confocal microscopy (SP-8 inverted confocal microscope, Leica microsystems, Wetzlar, Germany). Analysis was performed using Leica Application Suite X.

## 2.10. Ethics statement and preparation of hPCLS

Fresh human tissue taken from tumor resections was obtained from the CPC-M bioArchive at the Comprehensive Pneumology Center (CPC Munich, Germany). The study was approved by the local ethics committee of the Ludwig-Maximilians University of Munich, Germany (Ethic vote 19–630). Written informed consent was obtained for all study participants [18–20]. Briefly, PCLS were prepared from tumor-free peri-tumor tissue. The lung tissue was inflated with 3% agarose solution and solidified at 4 °C. Afterwards, 500 µm thick slices were cut from tissue blocks using a vibration microtome (HyraxV50) (Karl Zeiss AG, Oberkochen, Germany). PCLS were sliced and cultivated under submerged conditions in DMEM F-12 medium supplemented with 1% P/S, and 1% Ampicillin. For experiments, PCLS were cut by a biopsy puncher into slices of 6 mm diameter.

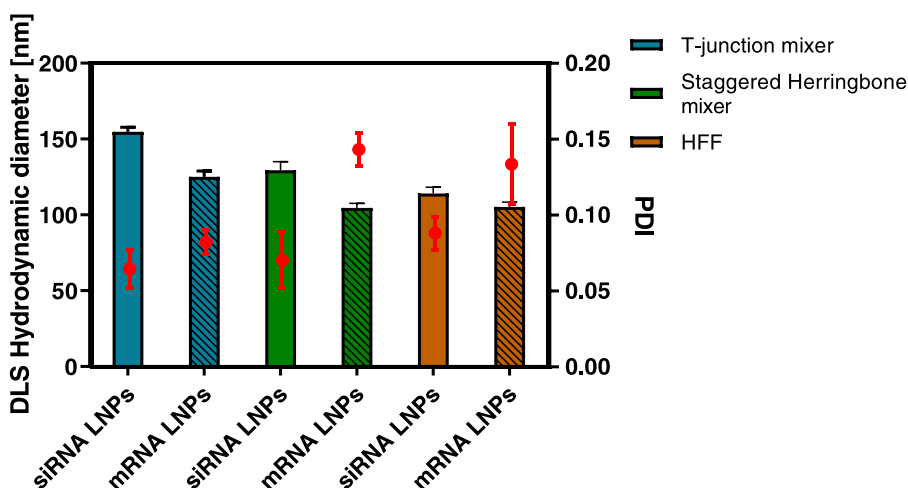


**Fig. 1.** Characterizing LNPs regarding hydrodynamic diameter, and polydispersity index (PDI). Hydrodynamic diameter and PDI were measured by DLS for siRNA and mRNA containing LNPs at pH 7.4 with 50 pmol siRNA at N/P ratio of 3 and 6, respectively. (Data indicate mean  $\pm$  SD,  $n = 3$ ).

### 2.11. PCLS knockdown

For GAPDH knockdown in precision cut lung slices (PCLS), two slices were placed in a 24-well plate supplied with 500  $\mu$ l DMEM F-12 medium (Sigma Aldrich, Taufkirchen, Germany) supplemented with 1% Penicillin-Streptomycin and 10% FBS. PCLS were transfected with 100 pmol GAPDH siRNA (Integrated DNA Technologies, Leuven, Belgium) LNPs or scrambled siRNA LNPs in duplicates. LNPs were formulated applying the HFF manufacturing method as described above. Experiments were conducted with tissue from one human donor. After 24 h, RNA was isolated according to an optimized protocol for PCLS [21]. cDNA synthesis was performed with a high-capacity cDNA synthesis kit (Applied Biosystems, Waltham, Massachusetts, USA). Afterward, cDNA was diluted 1:10 and qPCR was performed using the SYBR<sup>TM</sup> Green PCR master mix (Thermo Fisher Scientific, Darmstadt, Germany) with primers for GAPDH (Hs\_GAPDH\_2\_SG, Qiagen, Hilden, Germany) and  $\beta$ -actin (Hs\_ACTB\_2\_SG, Qiagen, Hilden, Germany) for normalization applying the  $\Delta\Delta$ Ct method. Amplification and data analysis was performed using a QuantStudio 3 Real-Time PCR (Thermo Fisher Scientific, Darmstadt, Germany). Cycle thresholds were acquired by autsetting with the qPCR software (Thermo Fisher Scientific, Darmstadt, Germany). Values are given as mean values  $\pm$  SEM.

Statistical Analysis: All experiments were performed in triplicates. All results are presented as mean value  $\pm$  standard deviation (SD). One-way ANOVA with Tuckey posthoc post-test was conducted in GraphPad Prism (GraphPad Software, La Jolla, USA) to calculate p-values with 95% confidence.

## 3. Results and discussion

### 3.1. Physico-chemical LNP characteristics

To investigate the feasibility of down-scaling the manufacturing process of siRNA- and mRNA-LNPs, we selected three different microfluidic mixing techniques based on common literature [5,22,23]. In particular, T-junction mixing, staggered Herringbone mixing, and microfluidic hydrodynamic flow focusing (HFF) were used with a total flow rate (TFR) as low as 5 ml/h. Reynolds numbers revealed values  $< 10$  in all geometries. As expected for the comparably low flow rates, the Reynolds Numbers calculated here indicate a controlled laminar flow regime within the microfluidic channels and, therefore, mixing primarily occurs through diffusion [24]. To ensure comparability between differently manufactured LNPs, other parameters such as lipid composition, lipid-to-RNA ratio (N/P ratio), buffer composition, TFR, FRR, and dialysis procedure were kept identical. Before evaluating *in vitro* efficiency, we focused on physicochemical LNP characteristics after dialysis and sterile filtration. Size measurements by dynamic light scattering (DLS) revealed that siRNA-, as well as mRNA-loaded LNPs, showed the largest hydrodynamic diameters with  $\sim 155$  and  $\sim 125$  nm, respectively, after T-junction mixing (Fig. 1). Larger sizes after T-junction mixing, however, were to some extent expected as a slow passing of the critical ethanol concentration for LNP formation has previously been shown by Maeki et al. to lead to the formation of larger LNPs [15]. Previous studies by Minakov et al. have shown that when operating a T-type micromixer at Reynolds numbers ( $Re$ ) within the range of  $5 < Re < 150$ , two symmetric horse-shoe vortices forms at the mixer entrance [25]. However, the T-junction mixer, which is known to exhibit suboptimal mixing efficiency in this mixing regime, may require higher flow rates to achieve optimal mixing performance, as observed by Ripoll and colleagues in their investigation of the influence of TFR on physico-chemical LNP properties in a ring micromixer used in Nanoassemblr<sup>®</sup> devices. Specifically, their findings indicated that at a TFR of 12 ml/min and a Reynolds number of 22, a side-by-side flow regime emerged within the microfluidic channel, leading to poor mixing and low homogeneity factor. As a result, they suggested that increasing the flow rate would be necessary to achieve optimal mixing and suitable particle sizes in the

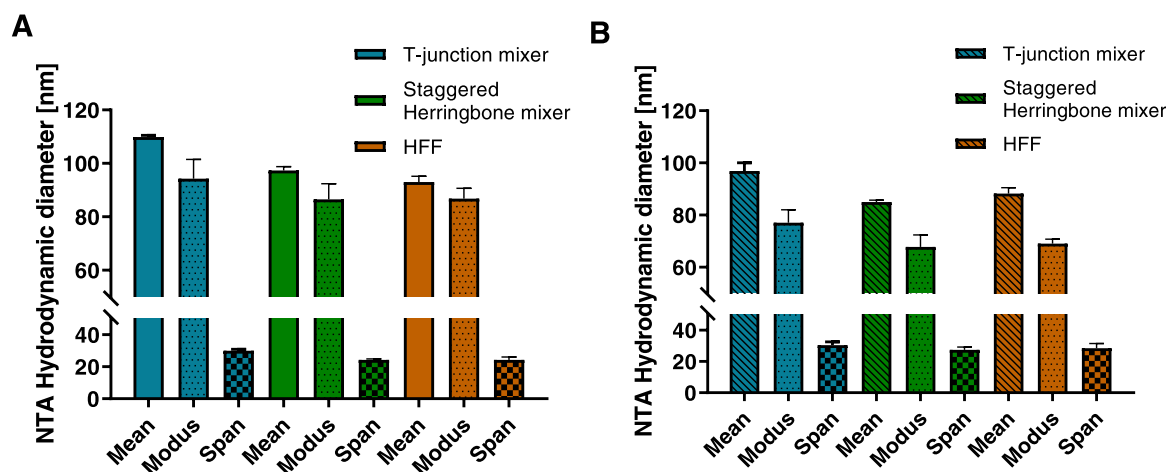


**Fig. 2.** Characterizing LNPs regarding hydrodynamic diameter. Mean, modus, standard deviation of hydrodynamic diameter were evaluated for siRNA (A) and mRNA (B) containing LNPs with nanoparticle tracking analysis (NTA) at pH 7.4 with 50 pmol siRNA at N/P ratio of 3 and 6, respectively. (Data indicates mean  $\pm$  SD,  $n = 3$ ).

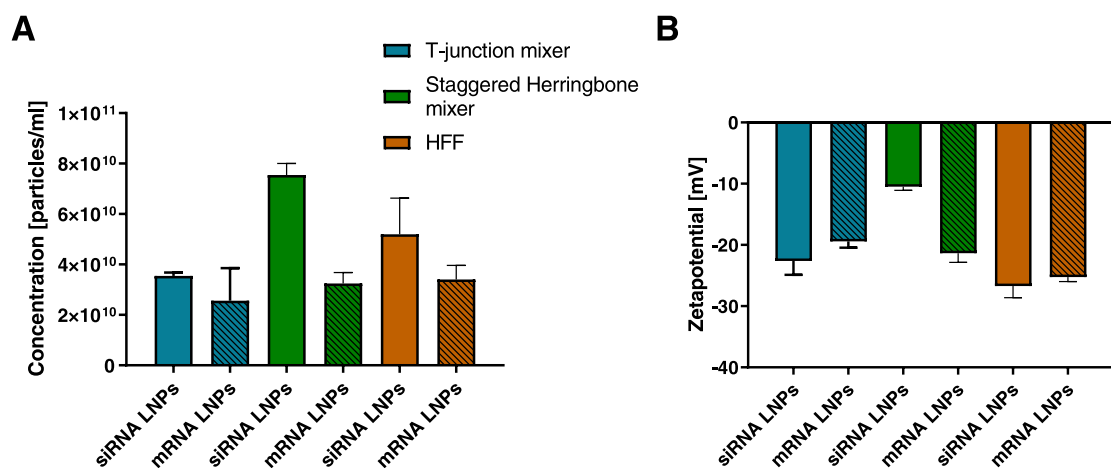


**Fig. 3.** Characterizing LNPs regarding particle concentration and zeta potential. Particle concentrations (A) of siRNA and mRNA LNPs at pH 7.4 with 50 pmol siRNA at N/P ratio of 3 and 6, respectively were evaluated with nanoparticle tracking analysis (NTA). Zeta potential (B) was evaluated via LDA at pH 7.4 for respective LNPs. (Data indicates mean  $\pm$  SD,  $n = 3$ ).

microfluidic unit [16]. We hypothesize that this phenomenon may also occur when using a T-mixer. For siRNA-loaded LNPs, the smallest size with  $\sim 114$  nm was achieved applying HFF. It has been shown that, when the middle fluid is injected at a lower flow rate, the other two solvents act as a sheath fluid, allowing for the compression of the middle fluid, resulting in reduced mixing time and improved particle uniformity by controlling solubility and concentration of the nanoparticle components [26]. Staggered Herringbone mixing led to intermediate-sized siRNA LNPs. We propose that Staggered Herringbone mixing facilitates effective mixing of the two fluids and hence leads to smaller LNPs. The microchannels in Herringbone mixers have grooves aligned diagonally, resulting in the development of vortices in the Herringbone grooves. Consequently, the mixing efficiency is improved compared to the simple T-junction mixing [27]. Formulating LNPs with mRNA showed smaller hydrodynamic diameters compared with the siRNA counterpart. Staggered Herringbone mixing as well as HFF-formulated LNPs had sizes of  $\sim 105$  nm. For mRNA LNPs, the size must take into consideration as Shepherd and colleagues showed that the administration of mRNA-loaded LNPs  $> 120$  nm led to variable *in vivo* activity whereas a stable mRNA expression was shown administrating  $< 85$  nm sized LNPs [10]. Regarding the particle size distribution in our study, all siRNA LNP formulations showed narrow size distribution with a PDI of  $< 0.1$ . For mRNA, surprisingly, the narrowest distribution (PDI  $< 0.1$ ) was measured after T-junction mixing. Staggered Herringbone mixing and HFF, however, led to average PDIs of 0.14 and 0.13, respectively. The particle sizes of siRNA and mRNA LNP formulations were overall larger compared with Onpatro-like LNPs formulated with commercially available systems [28]. Kon et al. formulated siRNA and mRNA LNPs with a Nanoassemblr® using a TFR of 12 ml/h for their studies on CCL cell transfection. The LNPs showed sizes of  $\sim 73$  nm using siRNA and  $\sim$

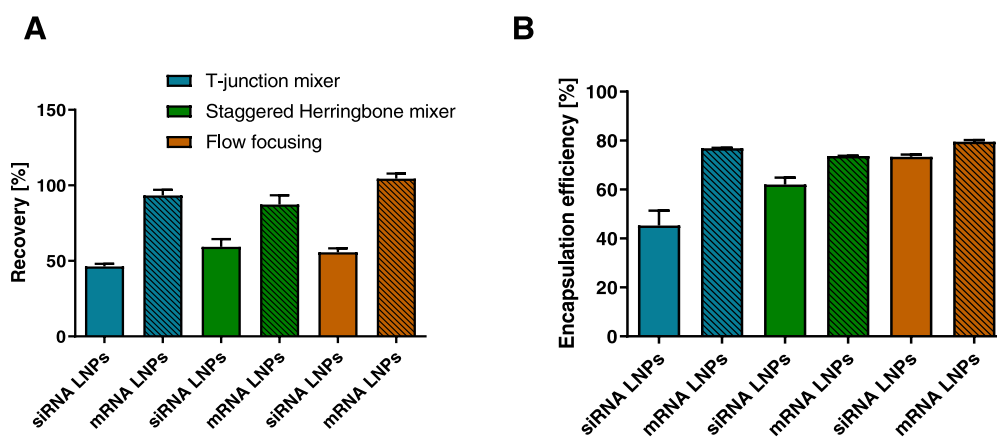


**Fig. 4.** Characterizing LNP towards overall recovery and encapsulation efficiency. For overall recovery (A) after dialysis and sterile filtration siRNA and mRNA containing LNPs were incubated for 1 h with 0.5% Triton-X 100 at 37 °C. For encapsulation efficiency (B) LNPs were diluted with TE-buffer. Both assays were analyzed after incubation for 10 min with RiboGreen assay reagent (1:100) with a plate reader. Standard curve was obtained in the respective buffer solution, separately. (Datapoints indicate mean  $\pm$  SD,  $n = 3$ ).

66 nm for mRNA-loaded LNPs [8]. Interestingly, a study performed by Basha et al. reported a particle size of  $< 40$  nm after the formulation of siRNA-loaded LNPs with a comparable lipid composition and a device provided by Precision NanoSystems [9]. Indeed, the use of higher flow rates and microfluidic channel geometry optimized for those flow conditions can decrease the LNP size. In this study, we have consciously decided to work with low flow rates and lipid concentrations. Hence, larger particle formation compared with the above-mentioned devices working with high TFR were expected as slower ethanol dilution was shown to increase LNP size [28].

We decided to further analyze the mean and modus of particle size by nanoparticle tracking analysis (NTA) [4,29]. NTA was chosen as it allows to evaluate particle distribution as number distribution derived from measuring individual particles whereas DLS provides an intensity distribution of the entire population. In this regard, Hassett et al. investigated the correlation between the different LNP biophysical characteristics by performing a Spearman correlation between NTA results and DLS data. They observed a correlation between the obtained size data, however, described that the results were not equal. Sizes measured by NTA for our formulations reflected overall slightly smaller hydrodynamic diameters with  $\sim 90$  nm to  $\sim 110$  nm (2 A and B) compared with DLS. The largest LNP mean size was found for siRNA LNPs with  $\sim 110$  nm and with  $\sim 100$  nm for mRNA LNPs after T-junction mixing which is in line with the trend seen in the DLS measurements. The smallest siRNA and mRNA LNPs could be obtained by applying HFF. Staggered Herringbone mixing led to an average of 5 nm larger LNPs for siRNA as well as for mRNA particles. The modus for siRNA LNPs differs by about 10 nm tending towards smaller nanoparticles. Interestingly, the mean and modus of mRNA LNPs differ to a greater extent compared with siRNA LNP although the overall size was smaller, indicating the start of aggregation processes (Fig. 2).

Notably, as seen in Fig. 3A the particle count for mRNA LNPs did not show differences across all mixing methods. In contrast, for siRNA LNPs, T-junction manufactured LNPs resulted in twice as many particles compared with staggered Herringbone mixing, possibly due to a lower particle loss within the microfluidic unit.

Next, the surface charge was evaluated. For zeta potential at a pH of 7.4, we expected a range of  $-4$  to  $-6$  mV, according to the literature [4]. LDA measurements, however, revealed surface charges in the range of  $-24$  mV to  $-8$  mV indicating free RNA in all formulations as shown in Fig. 3B. siRNA LNPs manufactured with staggered Herringbone mixing, however, showed the slightest deviation from the literature value. Thus, highest RNA encapsulation efficiency was expected. Furthermore, due to the electrostatic repulsion with the negatively charged cellular membrane, we expected lower uptake and knockdown efficiency of hydrodynamic flow focusing and T-junction manufactured LNPs [30].

### 3.1. Recovery and encapsulation efficiency

To determine the RNA loss during LNP formulation, buffer exchange, and sterile filtration we evaluated the overall recovery by RiboGreen assay after the addition of Triton-X 100. Ribogreen is a fluorescent dye emitting light if bound to free RNA. The highest recovery could be achieved for siRNA LNPs after T-junction mixing with  $\sim 60\%$  total recovery as shown in Fig. 4A. This might be attributed to the rather short channels of the T-Junction mixer and therefore less time and contact area for the formulation components to interact with the mixer's surface. The lowest RNA recovery for siRNA LNPs was measured at 46% using staggered Herringbone mixing. As this geometry exhibits the largest contact area and longest residence time of the fluid within the channels, this seems to support the observation with the T-Junction mixer. We observed a considerable loss of siRNA during the LNP formulation process, with a maximum recovery rate of 60%. However, it is worth noting that recovery values are infrequently reported in the literature, making it challenging to compare these results to those of other studies. We hypothesize that the loss of RNA during the LNP formulation process and encapsulation may be linked to the mixing regime of the RNA, as described for siRNA LNPs. For mRNA, surprisingly, a recovery of

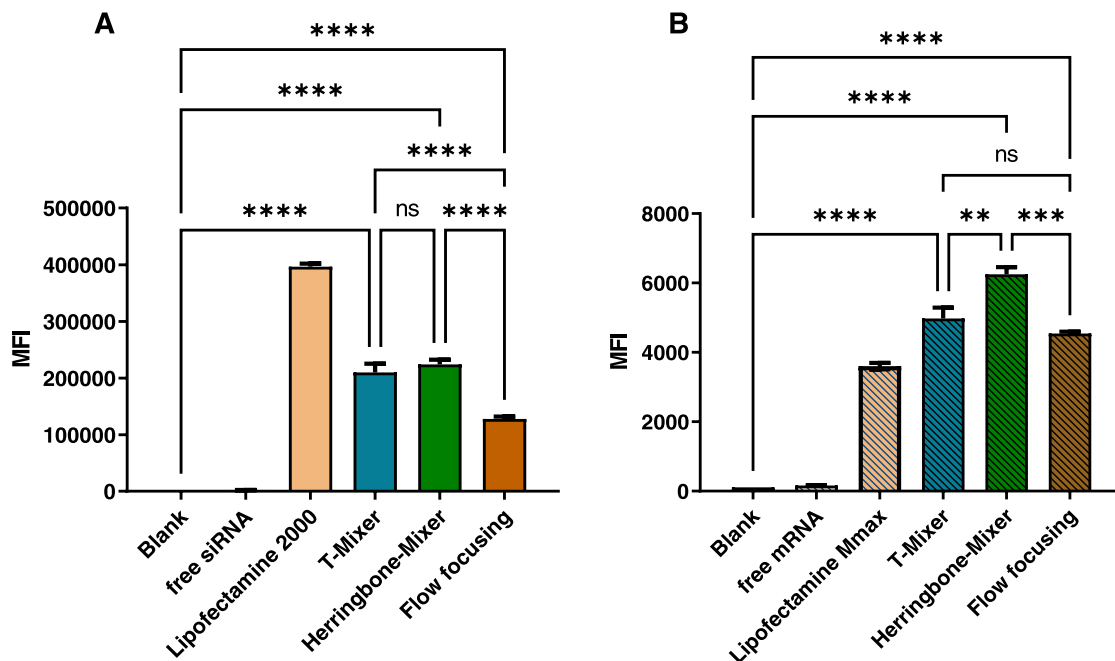


**Fig. 5.** Cellular uptake in H1299 cells after treatment with siRNA (A) or mRNA LNPs (B). For siRNA LNP cellular uptake cells were treated with LNPs containing 50 pmol AF488-labeled siRNA manufactured as described above at N/P 3 and analyzed by flow cytometry 24 h post transfection. Blank represents untreated cells. As positive control, 50 pmol of AF488-labeled siRNA was transfected with Lipofectamine 2000. For mRNA LNP cellular uptake, cells were treated with LNPs containing 100 ng Cy5-labeled eGFP mRNA manufactured as described above at N/P 6 and analyzed by flow cytometry 24 h post transfection. Blank represents untreated cells. As positive control, 100 ng of Cy5-labeled eGFP mRNA was transfected with Lipofectamine 2000. (Data points indicate mean  $\pm$  SD,  $n = 3$ ; One-way ANOVA, \*\*,  $p < 0.01$ , \*\*\*,  $p < 0.001$ , \*\*\*\*,  $p < 0.0001$ ).

94% for T-junction mixing, 97% for the staggered Herringbone mixer, and virtually full recovery for hydrodynamic flow focusing was achieved. Understanding those considerable differences between siRNA and mRNA recovery will certainly require in-depth analysis that goes beyond the scope of this study. One might however hypothesize that the ratio between drag forces caused by the fluid stream and adhesive forces of the RNA towards the wall might be favorable for mRNA due to its larger equivalent hydrodynamic diameter when compared to siRNA.

Next, we determined the amount of non-encapsulated RNA in the final formulations. Accordingly, we applied the same procedure without the addition of Triton-X 100 (Fig. 4B). As expected, when considering the negative zeta potentials, the encapsulation efficiency of siRNA LNPs was 45% to 73% depending on the mixing method used. In our study the best encapsulation efficiency was achieved after hydrodynamic flow-focusing formulation; the worst encapsulation was measured after T-junction mixing. Published siRNA LNP EE values usually are in a range of 80% to 95% depending on the used formulation method and lipid composition [28]. Therefore, with HFF an acceptable value for EE of siRNA LNP was achieved. Regarding mRNA EE, again, to our surprise, all mRNA formulations showed an encapsulation efficiency of about 80%, thus significantly outperforming their siRNA counterparts and matching most EE reported in literature [28].

### 3.2. Cellular uptake

To elucidate the influence of the mixing method on the cellular uptake, H1299 cells were treated for 24 h with LNPs encapsulating a dose of 50 pmol AF488-labeled siRNA (Fig. 5A) or 100 ng Cy5-labeled eGFP mRNA (Fig. 5B). A 24 h timepoint was chosen to ensure the cellular uptake as Gilleron and colleagues revealed that the cellular uptake of LNPs primarily happened within 6 h [31]. Before measurements, trypan blue was added after transfection with AF488-labeled siRNA to quench the fluorescence of non-internalized siRNA on the cell surface. Flow cytometry revealed similar median fluorescence intensity (MFI) of cells treated with siRNA LNPs manufactured by T-junction mixing or staggered Herringbone mixing. Cells treated with LNPs manufactured by hydrodynamic flow focusing, however, showed an MFI decreased by half. The reason for the difference in cellular uptake can be manifold. Gallud et al. showed that partial PEG shedding is one of the key factors enabling cellular LNP uptake [32]. In this regard, cellular uptake differences could be attributed to changes in LNP structure or lipid composition. Another explanation could be that the siRNA LNPs lost integrity before reaching the cells leading to decreased transfection efficiency of HFF produced LNPs. For mRNA, LNPs prepared through Herringbone mixing seem to be taken up slightly better. However, all mRNA formulations showed higher fluorescence values compared with Lipofectamine Mmax gold standard. It was observed that all siRNA and mRNA LNP formulations mediated considerable

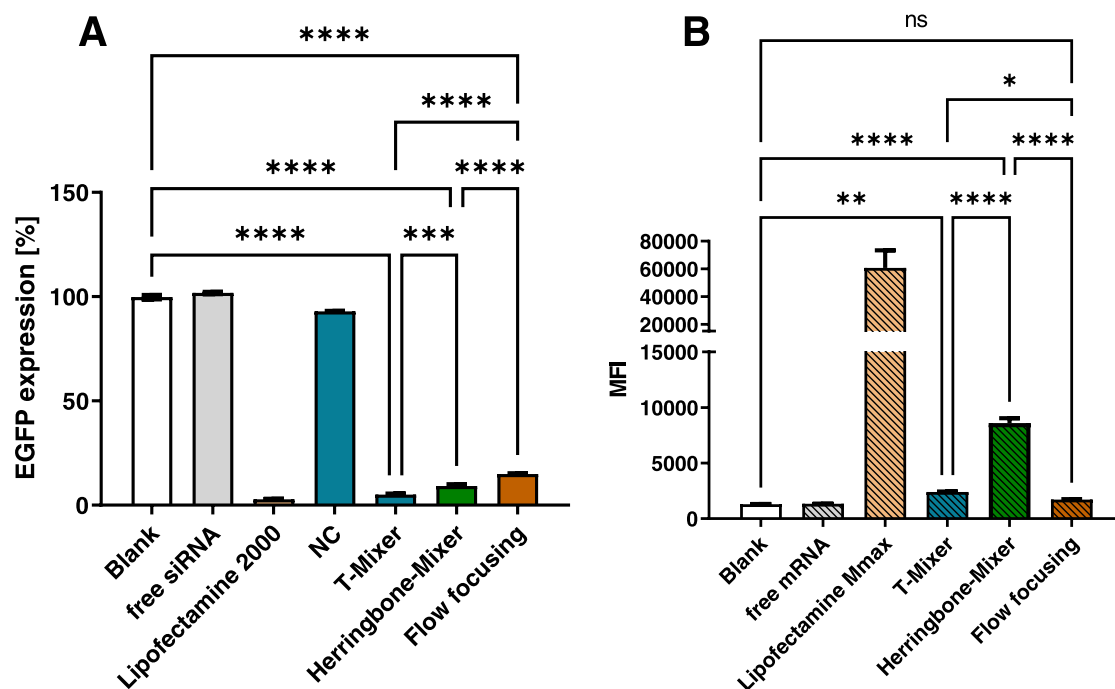


**Fig. 6.** GFP knockdown in H1299-GFP cells and eGFP expression in H1299 cells after treatment with siRNA (A) or mRNA LNPs (B). For GFP knockdown, H1299-GFP cells were treated with LNPs containing 50 pmol siGFP and scrambled siRNA (NC) at N/P 3 and analyzed by flow cytometry 48 h post transfection. eGFP expression of untreated H1299-GFP cells was used as 100% value. As positive control, 50 pmol of siRNA was transfected with Lipofectamine 2000. Blank represents untreated cells. For eGFP expression, H1299 cells were transfected with LNPs containing 100 ng eGFP mRNA at N/P 6 and analyzed 24 h post transfection with flow cytometry. Blank represents untreated cells. (Data points indicate mean  $\pm$  SD,  $n = 3$ ; One-way ANOVA, \*,  $p < 0.05$ , \*\*,  $p < 0.01$ , \*\*\*,  $p < 0.001$ , \*\*\*\*,  $p < 0.0001$ ).

cellular uptake regardless of their size, zeta potential, recovery, and encapsulation efficiency. This highlights the general efficacy of these formulations in facilitating cellular internalization. Of note, since LNPs are known to be taken up via apolipoprotein E (ApoE)-low density lipoprotein receptor (LDLR) and macropinocytosis pathway, these results are crucial for evaluating *in vitro* efficiency, however, are probably not transferable to the *in vivo* situation [31,33].

### 3.3. *In vitro* and *ex vivo* efficiency

The *in vitro* efficiency of the obtained LNPs was investigated by knocking down the GFP gene in eGFP expressing cells with siRNA and by eGFP expression induced through successful mRNA transfection, respectively. For these experiments, LNPs were loaded with 50 pmol GFP siRNA as described above. After 48 h of treatment with the respective formulations, the samples were analyzed by flow cytometry. As shown in Fig. 6A all siRNA formulations showed >90% GFP knockdown and are therefore comparable in activity with Lipofectamine 2000 positive control. The best GFP knockdown was achieved by T-junction mixed LNPs. Notably, the difference between T-junction mixed LNPs and flow-focusing manufactured LNPs was only around 5% even though the MFI of cellular uptake was approximately 50% lower. A possible explanation could be not only the lower cellular uptake of HFF prepared LNPs. For polymeric nanoparticle loaded with fluorescently labeled siRNA it was shown that depending on the fluorophore proximity the fluorescence can be quenched [34]. Thus, it is possible that HFF prepared LNPs encapsulate a higher number of siRNA per LNP. Importantly, all tested siRNA formulations displayed comparable knockdown efficiency to LNPs generated with higher flow rates, thus emphasizing the potential of the low flow rate procedure in producing LNPs with equivalent efficacy while simultaneously reducing costs and conserving materials. The knockdown efficiency of all siRNA LNP formulations is comparable with a recent study on GFP knockdown efficiency performed by Zimmermann et al. For testing GFP silencing capability in this study, -70 pmol eGFP siRNA was used encapsulated in various LNP formulations [35]. For evaluation of mRNA expression, H1299 wildtype were transfected with 100 ng eGFP mRNA and analyzed 24 h after transfection again by flow cytometry (Fig. 6B). The shorter incubation until evaluation compared with siRNA was used as expression onset time for a Dlin-MC3-DMA based LNP formulation was measured with about 1 h in HuH7 cells depending on the presence of serum [36]. Although cellular uptake experiments revealed that eGFP mRNA was taken up to a degree for all formulations, only the staggered Herringbone mRNA LNPs showed a significantly high mRNA expression after 24 h. However, mRNA expression was still very low compared with the Lipofectamine Mmax positive control. As cellular uptake and mRNA expression onset time was already exceeded, we hypothesize that mRNA LNP were not able to escape from the endosome, leading to decreased efficiency [36].

As the best results in terms of encapsulation efficiency for siRNA LNPs were achieved applying flow focusing, the cellular uptake

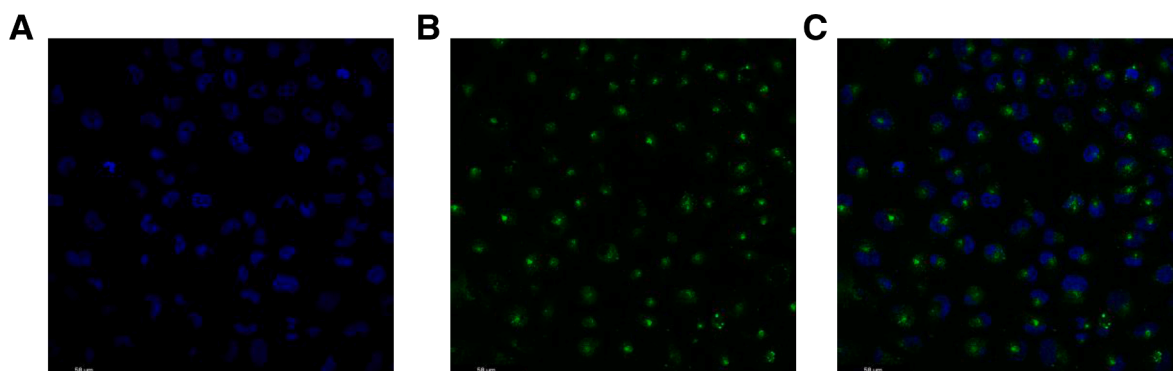


**Fig. 7.** Cellular uptake of siRNA in H1299 cells. H1299 cells were transfected with 50 pmol AF488 labeled siRNA and analyzed 24 h by confocal scanning microscopy after treatment. Blue represents nuclei stained with DAPI (A), green represents AF488-labeled siRNA (B). C represents merge picture.

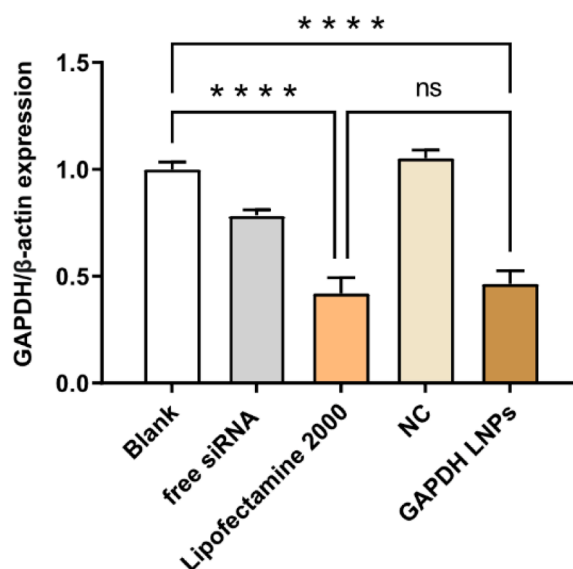


**Fig. 8.** GAPDH knockdown in PCLS treated with 100 pmol GAPDH containing LNPs at N/P 3. GAPDH expression was evaluated by qRT-PCR and normalized against  $\beta$ -actin expression applying  $2^{-\Delta\Delta Ct}$  method. Blank represents non-treated cells. Negative control (NC) cells were transfected with respective LNPs containing scrambled siRNA (Data points indicate mean  $\pm$  SD,  $n = 1$ ; One-way ANOVA, \*\*\*\*,  $p < 0.0001$ ).

performance was further verified by confocal microscopy as shown in Fig. 7 after 24 h.

To conclude whether siRNA-loaded LNPs manufactured by flow focusing are a promising formulation for pulmonary delivery to lung tissue, precision cut lung slices (PCLS) were transfected with 100 pmol of GAPDH siRNA-loaded LNPs. Zimmermann et al. showed that freshly prepared siGAPDH-loaded LNP can achieve an overall knockdown efficiency of approximately 50% in *ex vivo* lung tissue [35]. However, different LNP compositions were used in this study. As seen in Fig. 8 LNPs formulated by flow focusing lead to 50% silencing of GAPDH expression as reported earlier [35]. Moreover, the *ex vivo* silencing effect was not significantly different from Lipofectamine 2000 gold standard treated samples.

#### 4. Conclusion

In this study, we showed the feasibility of downscaling siRNA and mRNA LNP manufacturing with a TFR of 5 ml/h. LNPs formulated with T-junction mixing, staggered Herringbone mixing, and hydrodynamic flow focusing were physico-chemically characterized regarding hydrodynamic diameter, particle concentration, zeta potential, recovery, and encapsulation efficiency. As all formulated LNPs showed suitable characteristics for *in vitro* experiments, cellular uptake and EGFP knockdown or expression experiments were performed, respectively. LNPs loaded with siRNA showed significant cellular uptake and efficient gene knockdown. However, LNPs formulated with mRNA only mediated efficient gene expression efficacy after staggered Herringbone manufacturing. We further investigated siRNA LNPs prepared by HFF *ex vivo* as highest siRNA encapsulation efficiency was achieved. An GAPDH

knockdown in human precision cut lung slices (PCLS) revealed comparable knockdown efficiency with Lipofectamine gold standard. We conclude that siRNA LNPs manufactured by HFF at low flow rates and lipid concentration yield the best results among the tested mixing methods. This method allows to produce LNPs with small particle size and narrow size distribution, resulting in high *in vitro* and *ex vivo* efficiency, while simultaneously reducing material use and associated costs. Furthermore, our results indicate that HFF also leads to high overall recovery and encapsulation efficiency, highlighting its potential as a valuable tool for the development of siRNA LNPs on a lab-scale. For mRNA LNPs, however, only staggered Herringbone mixing led to a significant mRNA expression *in vitro*.

### CRedit authorship contribution statement

**David C. Jürgens:** Conceptualization, Methodology, Formal analysis, Investigation, Data curation, Writing – original draft, Visualization. **Leonie Defloch:** Methodology, Formal analysis, Investigation. **Diana Porras-Gonzalez:** Methodology, Investigation. **Joshua Winkeljann:** Methodology, Formal analysis, Investigation. **Sebastian Zielinski:** Methodology, Formal analysis, Investigation. **Matthias Munschauer:** Resources, Writing – review & editing. **Andreas L. Hörner:** Resources. **Gerald Burgstaller:** Resources, Writing – review & editing. **Benjamin Winkeljann:** Conceptualization, Methodology, Supervision, Supervision, Writing – review & editing. **Olivia M. Merkel:** Conceptualization, Methodology, Supervision, Resources, Project administration, Funding acquisition, Writing – review & editing.

### Declaration of Competing Interest

Olivia Merkel is a Scientific Board Member for Coriolis Pharma GmbH, AMW GmbH and Carver Biosciences and an Advisor for PARI Pharma GmbH, AbbVie Deutschland GmbH, and Boehringer-Ingelheim International GmbH.

### Acknowledgments

B.W. and J.W. acknowledge the Center of Nanoscience (CeNS) Munich for financial support for joint research projects. M.M. and O. M.M. acknowledge the broad-spectrum antivirals challenge of the Federal Agency for Disruptive Innovation (SPRIND) under grant "BacDefense" for financial support. We gratefully acknowledge the provision of human biomaterial (fresh human peritumor tissue) and clinical data from the CPC-M bioArchive and its partners at the Asklepios Biobank Gauting, the LMU Hospital and the Ludwig-Maximilians-Universität München. We thank the patients and their families for their support.

### Supplementary materials

Supplementary material associated with this article can be found, in the online version, at [doi:10.1016/j.onano.2023.100161](https://doi.org/10.1016/j.onano.2023.100161).

### References

- [1] B. Hu, et al., Therapeutic siRNA: state of the art, *Signal Transduct. Target. Ther.* 5 (1) (2020) 101.
- [2] L. Schoenmaker, et al., mRNA-lipid nanoparticle COVID-19 vaccines: structure and stability, *Int. J. Pharm.* 601 (2021), 120586.
- [3] C. Webb, et al., Current status and future perspectives on mRNA drug manufacturing, *Mol. Pharm.* 19 (4) (2022) 1047–1058.
- [4] M.J. Carrasco, et al., Ionization and structural properties of mRNA lipid nanoparticles influence expression in intramuscular and intravascular administration, *Commun. Biol.* 4 (1) (2021) 956.
- [5] C.B. Roces, et al., Manufacturing considerations for the development of lipid nanoparticles using microfluidics, *Pharmaceutics* 12 (11) (2020) 1095.
- [6] T. Terada, et al., Characterization of lipid nanoparticles containing ionizable cationic lipids using design-of-experiments approach, *Langmuir* 37 (3) (2021) 1120–1128.
- [7] E. Kenjo, et al., Low immunogenicity of LNP allows repeated administrations of CRISPR-Cas9 mRNA into skeletal muscle in mice, *Nat. Commun.* 12 (1) (2021) 7101.
- [8] E. Kon, et al., Resveratrol enhances mRNA and siRNA lipid nanoparticles primary CLL cell transfection, *Pharmaceutics* 12 (6) (2020) 520.
- [9] G. Basha, et al., Influence of cationic lipid composition on gene silencing properties of lipid nanoparticle formulations of siRNA in antigen-presenting cells, *Mol. Ther.* 19 (12) (2011) 2186–2200.
- [10] S.J. Shepherd, et al., Scalable mRNA and siRNA lipid nanoparticle production using a parallelized microfluidic device, *Nano Lett.* 21 (13) (2021) 5671–5680.
- [11] S.Z. Mirjalili Mohanna, et al., LNP-mediated delivery of CRISPR RNP for wide-spread *in vivo* genome editing in mouse cornea, *J. Control. Release* 350 (2022) 401–413.
- [12] A. Akinc, et al., The Onpatro story and the clinical translation of nanomedicines containing nucleic acid-based drugs, *Nat. Nanotechnol.* 14 (12) (2019) 1084–1087.
- [13] C. Hald Albertsen, et al., The role of lipid components in lipid nanoparticles for vaccines and gene therapy, *Adv. Drug Deliv. Rev.* 188 (2022), 114416.
- [14] A. Sarode, et al., Predictive high-throughput screening of PEGylated lipids in oligonucleotide-loaded lipid nanoparticles for neuronal gene silencing, *Nanoscale Adv.* 4 (9) (2022) 2107–2123.
- [15] M. Maeki, et al., Understanding the formation mechanism of lipid nanoparticles in microfluidic devices with chaotic micromixers, *PLoS One* 12 (11) (2017), e0187962.
- [16] M. Ripoll, et al., Optimal self-assembly of lipid nanoparticles (LNP) in a ring micromixer, *Sci. Rep.* 12 (1) (2022) 9483.
- [17] D.E. Jeong, M. McCoy, K. Artilles, O. Ilbay, A. Fire, K. Nadeau, H. Park, B. Betts, S. Boyd, R. Hoh, et al., Assemblies of Putative SARS-CoV2 Spike Encoding mRNA Sequences for Vaccines BNT-162b2 and mRNA-1273. Available online: <https://virological.org/t/assemblies-of-putative-sars-cov2-spike-encoding-mrna-sequences-for-vaccines-bnt-162b2-andmna-1273/663> (Accessed 09 May 2023).
- [18] M. Gerckens, et al., Generation of human 3D lung Tissue cultures (3D-LTCs) for disease modeling, *J. Vis. Exp.* 144 (2019) 1–8.

- [19] H.N. Alsafadi, et al., An *ex vivo* model to induce early fibrosis-like changes in human precision-cut lung slices, *Am. J. Physiol. Lung Cell. Mol. Physiol.* 312 (6) (2017) L896–L902.
- [20] S. Ambike, et al., Targeting genomic SARS-CoV-2 RNA with siRNAs allows efficient inhibition of viral replication and spread, *Nucleic Acids Res.* (2021) 1–17.
- [21] M. Niehof, et al., RNA isolation from precision-cut lung slices (PCLS) from different species, *BMC Res. Notes* 10 (1) (2017) 121.
- [22] N.N. Zhang, et al., A thermostable mRNA vaccine against COVID-19, *Cell* 182 (5) (2020) 1271–1283, e16.
- [23] N.M. Belliveau, et al., Microfluidic synthesis of highly potent limit-size lipid nanoparticles for *in vivo* delivery of siRNA, *Mol. Ther. Nucleic Acids* 1 (2012) e37.
- [24] N. Convery, N. Gadegaard, 30 Years of microfluidics, *Micro Nano Eng.* 2 (2019) 76–91.
- [25] A. Minakov, et al., Investigation of slip boundary conditions in the T-shaped microchannel, *Int. J. Heat Fluid Flow* 43 (2013) 161–169.
- [26] M. Lu, et al., Microfluidic hydrodynamic focusing for synthesis of nanomaterials, *Nano Today* 11 (6) (2016) 778–792.
- [27] M.S. Williams, K.J. Longmuir, P. Yager, A practical guide to the staggered herringbone mixer, *Lab Chip* 8 (7) (2008) 1121–1129.
- [28] M. Maeki, et al., Microfluidic technologies and devices for lipid nanoparticle-based RNA delivery, *J. Control. Release* 344 (2022) 80–96.
- [29] K.J. Hassett, et al., Impact of lipid nanoparticle size on mRNA vaccine immunogenicity, *J. Control. Release* 335 (2021) 237–246.
- [30] Y. Ge, et al., Effect of surface charge and agglomerate degree of magnetic iron oxide nanoparticles on KB cellular uptake *in vitro*, *Colloids Surf. B Biointerfaces* 73 (2) (2009) 294–301.
- [31] J. Gilleron, et al., Image-based analysis of lipid nanoparticle-mediated siRNA delivery, intracellular trafficking and endosomal escape, *Nat. Biotechnol.* 31 (7) (2013) 638–646.
- [32] A. Gallud, et al., Time evolution of PEG-shedding and serum protein coronation determines the cell uptake kinetics and delivery of lipid nanoparticle formulated mRNA, *Biorxiv* (2021), <https://doi.org/10.1101/2021.08.20.457104>.
- [33] Y. Sato, et al., Different kinetics for the hepatic uptake of lipid nanoparticles between the apolipoprotein E/low density lipoprotein receptor and the N-acetyl-D-galactosamine/asialoglycoprotein receptor pathway, *J. Control. Release* 322 (2020) 217–226.
- [34] M. Zheng, et al., Targeting the blind spot of polycationic nanocarrier-based siRNA delivery, *ACS Nano* 6 (11) (2012) 9447–9454.
- [35] C.M. Zimmermann, et al., Spray drying siRNA-lipid nanoparticles for dry powder pulmonary delivery, *J. Control. Release* 351 (2022) 137–150.
- [36] A. Reiser, et al., Correlation of mRNA delivery timing and protein expression in lipid-based transfection, *Integr. Biol.* 11 (9) (2019) 362–371 (Camb).